ELSEVIER

Valence state and spin transitions of iron in Earth's mantle silicates

Feiwu Zhang *, Artem R. Oganov

Laboratory of Crystallography, Department of Materials, ETH Zurich, Wolfgang-Pauli-Strasse 10, CH-8093, Zurich, Switzerland

Abstract

Using *ab initio* simulations, we investigated the valence and spin states of iron impurities in the perovskite (Pv) and post-perovskite (PPv) polymorphs of $MgSiO_3$. In agreement with the previous experimental work, we find a valence disproportionation reaction: $3Fe^{2+} \rightarrow 2Fe^{3+} Fe^0_{metal}$. This exothermic reaction results in the predominance of Fe^{3+} impurities in lower mantle silicates and produces free metallic iron. It occurs both in Pv and PPv, Al-free and Al-rich, at all lower mantle pressures. This reaction provides a possible mechanism for the growth of the Earth's core and core-mantle chemical equilibration. In the presence of Al^{3+}, iron forms $Fe^{3+}–Al^{3+}$ coupled substitutions in Pv, but separate $Fe^{3+}-Fe^{3+}$ and $Al^{3+}-Al^{3+}$ substitutions in PPv. Only the high-spin state is found for Fe^{2+} impurities at all mantle pressures, while Fe^{3+} impurities on the Si-site are low-spin at all pressures in both phases. Fe^{3+} impurities on the Mg-site are in the high-spin state in PPv at all mantle pressures, but in Pv we predict a high-spin–low-spin transition. The pressure at which this transition occurs strongly depends on the Al^{3+} content and according to our calculations increases from 76 GPa for Al-free to 134 GPa for aluminous Pv; this reconciles many of the previous experimental results. Our findings have implications for the chemical evolution of the Earth and for the radiative conductivity and dynamics of the D" layer.
© 2006 Elsevier B.V. All rights reserved.

Keywords: valence state of iron; spin transitions of iron; Earth's mantle; D" layer; perovskite; post-perovskite; substitution mechanism; *ab initio* simulations

1. Introduction

Earth's lower mantle is believed to contain ∼75 vol.% $(Mg,Fe)SiO_3$ perovskite, 20 vol.% $(Mg,Fe)O$ ferropericlase, 5 vol.% $CaSiO_3$ perovskite. In the lowermost ∼200 km of the mantle, $(Mg,Fe)SiO_3$ adopts the post-perovskite structure. While the properties and behaviour of pure $MgSiO_3$ phases are mostly understood, the effects of impurities — most importantly iron and aluminium, are poorly known and the existing experimental studies are contradictory.

Iron is the most abundant transition-metal element in the Earth — most of it is in the Earth's core, but a significant amount is in the form of impurities in mantle silicates and oxides. Valence and spin state of the iron impurities determines many properties of the Earth's mantle minerals [1–5] (thermal and electrical conductivities, rheology, thermodynamics, etc.), in particular of $MgSiO_3$ perovskite (Pv) and post-perovskite (PPv) [6,7]. While in low-pressure magnesium silicates (e.g., olivines, pyroxenes) high-spin (HS) Fe^{2+} is dominant, recent high-pressure experiments demonstrated dramatic

* Corresponding author. Tel.: +41 44 632 3056; fax: +41 44 632 1133.
  E-mail address: feiwu.zhang@mat.ethz.ch (F. Zhang).

changes in *Pv*, with implications for the dynamics and chemical evolution of the Earth [3–5,8]. Badro et al. [4] have observed a spin transition of iron in *Pv* and speculated that this could enhance the radiative conductivity of the D'' layer and lead to the formation of a non-convective layer at the bottom of the mantle; subsequent studies of this spin transition performed by different groups [9–11] appeared to be rather discrepant.

Frost et al. [3,5] found disproportionation of Fe^{2+} into Fe^{3+} and metallic iron at lower mantle conditions, with *Pv* having the $Fe^{3+}/\Sigma Fe$ ratio of at least 0.6. On the basis of their experiments, Sinmyo et al. [12] reached similar conclusions for *PPv*. Little is known about the thermodynamics of this counterintuitive coexistence of Fe^{3+} impurities in *Pv* and *PPv* and metallic iron.

One of the widely discussed questions was the effect of Al^{3+} on iron incorporation in *Pv* and *PPv*. It is well known that even a small amount of Al^{3+} can radically change Fe–Mg partitioning and phase equilibria [1] between lower mantle minerals, leading to a significant enrichment of *Pv* in Fe^{3+} [2]. Not much is known about the effects of Fe^{2+}, Fe^{3+} and Al^{3+} impurities on the newly discovered *PPv* [6,7]. Yet, the effects of impurities on mineral properties (both for *Pv* and *PPv*) must be addressed in order to obtain realistic physical and chemical models of the Earth's mantle.

Since direct experimental studies are difficult and have resulted in discrepant results [4,9,11], here we perform an extensive study using *ab initio* calculations. We have obtained results concerning (i) the valence state of iron impurities, (ii) the mechanisms of Al^{3+}, Fe^{2+} and Fe^{3+} substitutions, (iii) and the spin state of iron (Fe^{2+} and Fe^{3+}) in both $MgSiO_3$ phases. Section 2 describes the computational methodology used in this work, the results of simulations will be discussed in Section 3. Section 4 gives a brief summary of this work.

2. Computational methodology

Our *ab initio* simulations are based on density functional theory within the generalized gradient approximation (GGA) [13] and using the all-electron PAW method [14,15] as implemented in the VASP code [16]. The PAW potentials that we used have $1s^2 2s^2$ core (radius 2 a.u.) for Mg, $1s^2 2s^2 2p^6$ core (radius 1.5 a.u.) for Si, $1s^2$ core (radius 1.52 a.u.) for O, $1s^2 2s^2 2p^6$ core (radius 1.9 a.u.) for Al and $1s^2 2s^2 2p^6 3s^2$ core (radius 2.2 a.u.) for Fe. We have used the plane-wave cut-off of 500 eV for representing the wave functions and the Γ-point for the Brillouin zone sampling. All our calcula-

tions used 160-atom supercells. Our computational settings enable convergence of the energy differences to 0.004 meV/atom, compressional stresses to 0.1 GPa and shear stresses to 0.5 GPa. Structural relaxation was done using the conjugate-gradients method, until the total energy changes were below 10^{-4} eV.

Due to incomplete account of on-site Coulomb correlations, the GGA often incorrectly describes the electronic structure of Fe^{2+}-containing materials; still, it gives a good description of their equations of state [17] and for compounds of Fe^{3+} and metallic iron, the GGA is also capable of producing correct electronic structures. To check the effects of on-site electron correlations for iron 3d-electrons, we performed tests using the GGA+U method [18] with U–J=4.0 eV — they produced the same preferred spin states as found using the GGA. U–J is an empirical parameter depending on the oxidation state of iron atoms (e.g. it is known to be much less important for Fe^0 and Fe^{3+} than for Fe^{2+}), which prevented us from using this approach for oxidation–reduction reactions. Therefore, below we discuss only the GGA results.

Due to major difficulties in performing *ab initio* calculations on spin systems at finite temperature, all calculations presented here were done at 0 K. With the help of simple statistical mechanics, it is possible to discuss the effects of temperature on our results (see Supplementary material for details).

To study the effects of substitutions, we introduced one defect unit (Fe^{2+}, Fe^{3+} or coupled defects [Fe^{3+}–Al^{3+}], [Al^{3+}-Al^{3+}] and [Fe^{3+}-Fe^{3+}]) into 160-atom *Pv* and *PPv* supercells. Several coupled substitution mechanisms could be imagined for the incorporation of Fe^{3+} and Al^{3+} into *Pv* and *PPv* phase of $MgSiO_3$. The first one is a coupled isosubstitution $2M^{3+} \rightarrow M^{\bullet}_{Mg} + M'_{Si}$ [19], where the same impurity atom M enters both cation sites (M^{3+} can stand for either Fe^{3+} or Al^{3+}, $\bullet$ and $'$ superscripts represent a positive or negative net charge on the site, respectively.) The second mechanism is a coupled heterosubstitution, where Al^{3+} and Fe^{3+} jointly enter the neighbouring Mg and Si-sites — as in either $(Mg,Fe)(Si,Al)O_3$ or $(Mg,Al)(Si,Fe)O_3$ [2,3,8]. Substitutions by oxygen-vacancy mechanism (OVM) could also exist [19], e.g. $2Al^3 \rightarrow 2Al_{Si} + V_{\ddot{O}}$ (where $V_{\ddot{O}}$ denotes an oxygen vacancy). Previous experimental [2,3,8] and theoretical [19] studies have demonstrated that coupled substitutions $(Mg,Fe)(Si,Al)O_3$ and $(Mg,Al)(Si,Al)O_3$ are preferred in *Pv*, while the OVM for Al^{3+} is energetically unfavourable (our calculations show that Fe^{3+}-Fe^{3+} and Fe^{3+}–Al^{3+} types of the OVM are also unfavourable). We take the nearest neighbor sites for coupled impurities, which emerged as

energetically the most energetically favorable configuration in all previous theoretical studies [10], except Al^{3+}-Al^{3+} substitution in PPv, for which we found a slightly more favourable configuration.

3. Results and discussion

First, we calculated the enthalpies of all the substitution possibilities of Al^{3+}, Fe^{2+} and Fe^{3+} impurities both in Pv and PPv (Table 1), as well as all the spin state possibilities of Fe^{2+}–Fe^{3+} ions at 100 GPa. In order to evaluate the thermodynamics of the Al^{3+} incorporation into MgSiO$_3$ PPv, we have studied the following reaction:

$$Mg_{33}(Si_{31}Al_2)O_{98} = (Mg_{31}Al)(Si_{31}Al)O_{96} + 2MgO$$

(1)
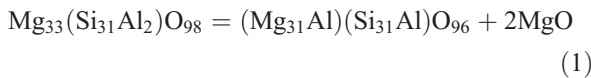
Eq. (1) represents the reaction from an oxygen-vacancy (OVM) substitution to charge coupled (CCM) substitution. The calculated reaction enthalpies ΔH are −5.169 eV at 100 GPa and −6.247 eV at 150 GPa, which means that Al^{3+} ions strongly prefer to be incorporated into PPv through CCM, and therefore there is no need for oxygen vacancies. The Al substitution mechanism in Pv [1,3,8,19] is similar, with OVM unfavorable above ∼30 GPa [19]. Even though at high pressures Al$_2$O$_3$ adopts the CaIrO$_3$-type PPv structure, the Al$_2$O$_3$ component prefers to dissolve preferentially in the Pv phase [20–22].

From Table 1, it is very clear that Fe^{2+} is in the HS state in both (Mg,Fe)SiO$_3$ Pv and PPv at 100 GPa; in agreement with previous studies [11,17,20] the spin state does not change at least up to 150 GPa. Therefore,

the spin transition observed experimentally [4,9,11] is more likely to be associated with Fe^{3+}.

Considering Fe^{3+}–Al^{3+} coupled substitutions, in agreement with recent experimental results [23], (Mg, Fe)(Si,Al)O$_3$ with Fe^{3+} occupying the Mg-site and Al^{3+} occupying the Si-site is always more energetically favourable than (Mg,Al)(Si,Fe)O$_3$ for both Pv and PPv, which is readily explained by ionic sizes.

Fe^{3+} in aluminous Pv (Mg,Fe)(Si,Al)O$_3$ has a HS–LS transition at 134 GPa (cf. 105 GPa found in recent simulations [10]). For Al-free Pv (Mg,Fe)(Si,Fe)O$_3$, we find a HS–LS transition of Fe^{3+} in the Mg-site at ∼76 GPa (Fig. 1), which is consistent with the pressure of 70 GPa suggested by some experiments [4,11].

At the same time, in (Mg,Fe)(Si,Fe)O$_3$ PPv, there is no spin transition at all mantle pressures, consistent with Stackhouse et al. [24]. In this case, Fe^{3+} in the Mg-site is always in the HS state, whereas Fe^{3+} in the Si-site is always in the LS state. As we show below, in PPv Al^{3+} and Fe^{3+} impurities are decoupled from each other and separator [Al^{3+}–Al^{3+}] and [Fe^{3+}–Fe^{3+}] substitutions are more favourable than [Fe^{3+}–Al^{3+}] substitutions. Therefore, even in presence of moderate concentrations of Al^{3+} the situation will not change and there will be no spin transition in PPv at Earth's mantle pressures.

We find that for Fe^{3+} in the Si-site, the LS state is preferred, in both MgSiO$_3$ polymorphs at all relevant pressures. This is explained by the strong crystal field on this small cationic site.

To explore the chemistry of Fe-substitutions in the MgSiO$_3$ phases, we considered a number of reactions given below (for each reaction we give the enthalpy in eV at 100 GPa, one value for the Pv structure of

Table 1
Defect incorporation enthalpies ΔH (eV) in Pv and PPv at 100 GPa [a]

MgSiO$_3$	(Mg,Al)(Si,Al)O$_3$ [Al^{3+}-Al^{3+}]	(MgFe)SiO$_3$ Fe^{2+}	(Mg,Al)(Si,Fe)O$_3$ [b] [Al^{3+}–Fe^{3+}]	(Mg,Fe)(Si,Al)O$_3$ [Fe^{3+}–Al^{3+}]	(Mg,Fe)(Si,Fe)O$_3$ [Fe^{3+}-Fe^{3+}]
Pv	−0.774	−1.561 (HS) −0.225 (LS)	0.630 (LS) 0.857 (NM)	−0.003 (HS) 0.187 (IS) 0.248 (LS) 0.642 (NM)	1.091 (HS–LS) fm 1.139 (IS–LS) 1.053 (LS–LS) 1.058 (NM)
PPv	−0.509	−1.802 (HS) −0.154 (LS)	0.170 (LS) 0.474 (NM)	0.025 (HS) 0.380 (IS) 0.981 (LS) 1.350 (NM)	0.193 (HS–LS) afm 0.037 (HS–LS) fm 1.550 (NM)

[a] The calculated enthalpy differences of possible substitutions of Al^{3+}, Fe^{2+} and Fe^{3+} impurities in Pv and PPv. Extensive calculations were performed starting with different spin states; here we show the final spin states: HS, which is 5 μB for Fe^{3+} and 4 μB for Fe^{2+}, intermediate spin (IS), which is 3 μB for Fe^{3+} and 2 μB for Fe^{2+}, LS, which is 1 μB for Fe^{3+} and 0 for Fe^{2+}. NM — non-magnetic calculation. "fm" and "afm" indicate parallel or antiparallel orientation of spins on the neighbouring iron atoms. The reported ΔH values are per defect unit and were calculated as the difference between the enthalpies of the pure phase (Pv or PPv) and its impurity-bearing counterpart.

[b] HS and IS of Fe are unstable in (Mg,Al)(Si,Fe)O$_3$, they revert to LS after optimization.

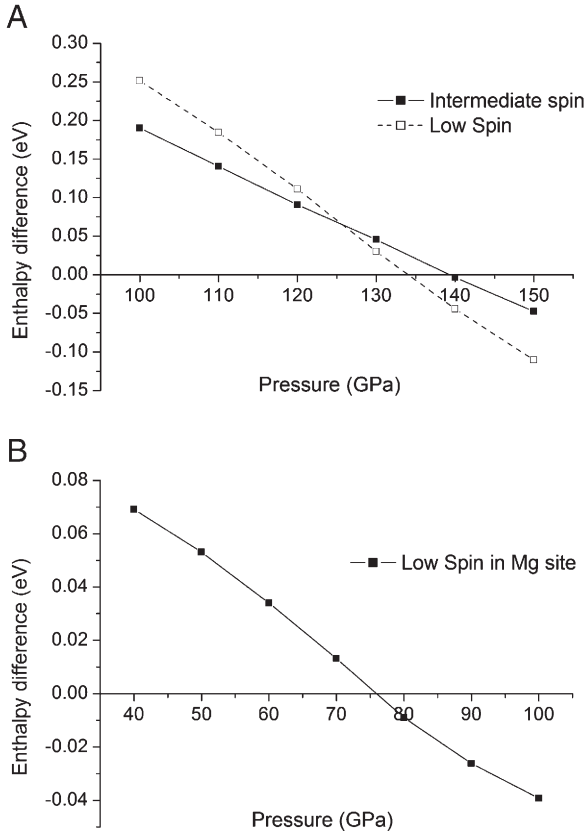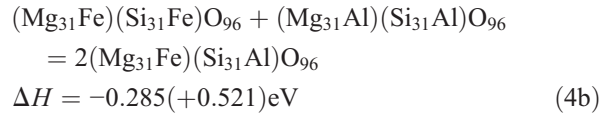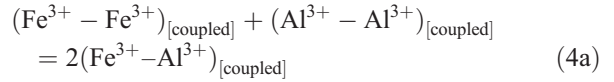Fig. 1. Spin transitions in *Pv*: (A) enthalpies of IS and LS states relative to the HS state in $(Mg,Fe)(Si,Al)O_3$ *Pv* as a function of pressure, showing a HS–LS transition in the Al-bearing system at 134 GPa, (B) enthalpy of the LS state relative to the HS state for Fe^{3+} in the Mg-site of $(Mg,Fe)(Si,Fe)O_3$ *Pv*, showing a HS–LS transition in the Al-free system at 76 GPa (on the Si-site Fe^{3+} is always LS — see text).

$MgSiO_3$, the other, in parentheses — for the *PPv* structure):

$$3Fe^{2+} = Fe + (Fe^{3+} - Fe^{3+})_{[coupled]} \tag{2a}$$

$$3(Mg_{31}Fe)Si_{32}O_{96} = (Mg_{93}Fe)(Si_{93}Fe)O_{282}$$
$$+ Fe + 3SiO_2$$
$$\Delta H = -2.266(-2.575)eV \tag{2b}$$
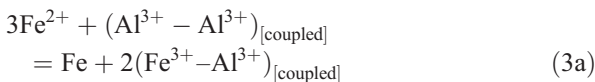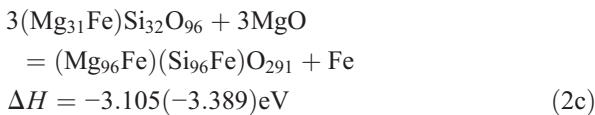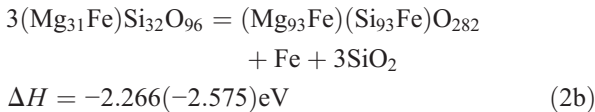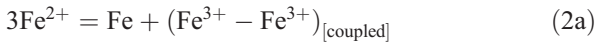
$$3(Mg_{31}Fe)Si_{32}O_{96} + 3MgO$$
$$= (Mg_{96}Fe)(Si_{96}Fe)O_{291} + Fe$$
$$\Delta H = -3.105(-3.389)eV \tag{2c}$$

$$3Fe^{2+} + (Al^{3+} - Al^{3+})_{[coupled]}$$
$$= Fe + 2(Fe^{3+} - Al^{3+})_{[coupled]} \tag{3a}$$

$$3(Mg_{31}Fe)Si_{32}O_{96} + (Mg_{31}Al)(Si_{31}Al)O_{96}$$
$$= 2(Mg_{62}Fe)(Si_{62}Al)O_{189} + Fe + 3SiO_2$$
$$\Delta H = -2.551(-2.054)eV \tag{3b}$$

$$3(Mg_{31}Fe)Si_{32}O_{96} + (Mg_{31}Al)(Si_{31}Al)O_{96} + 3MgO$$
$$= (Mg_{127}Fe_2)(Si_{127}Al_2)O_{387} + Fe$$
$$\Delta H = -3.390(-2.868)eV \tag{3c}$$

$$(Fe^{3+} - Fe^{3+})_{[coupled]} + (Al^{3+} - Al^{3+})_{[coupled]}$$
$$= 2(Fe^{3+} - Al^{3+})_{[coupled]} \tag{4a}$$

$$(Mg_{31}Fe)(Si_{31}Fe)O_{96} + (Mg_{31}Al)(Si_{31}Al)O_{96}$$
$$= 2(Mg_{31}Fe)(Si_{31}Al)O_{96}$$
$$\Delta H = -0.285(+0.521)eV \tag{4b}$$

Eqs. (2a) (3a) (4a) give generalized chemical reactions of each type. Reactions with an excess of either MgO or SiO_2 are relevant for different regions of the lower mantle characterized by different mineralogy (e.g. 2b *vs* 2c, 3b *vs* 3c.) – for instance, the SiO_2 – excess reaction may be relevant for silica-rich parts of subducted slabs. These chemical reactions are inter-related: (2c) minus (2b) and (3c) minus (3b) are simply reactions describing the formation of the $MgSiO_3$ phases from the component binary oxides, whereas (4b) = (3b) − (2b) describes the energetics of the ordering of Fe^{3+} and Al^{3+} ions between the Si and Mg-sites. We note that our calculated reaction enthalpies included the effect of phase transitions in the relevant materials: for SiO_2, stishovite and $CaCl_2$-type [25] structure below 98 GPa and α-PbO_2-type [26] structure above 100 GPa; for iron above 13 GPa we considered the non-magnetic *hcp*-Fe, which is known [27] to be stable at these conditions.

Recent experiments showed that free metallic iron can coexist in the Earth's lower mantle with ferric iron-rich *Pv* [3,5] and *PPv* [12], at least in presence of alumina in the system. Indeed, the enthalpies of reactions (Fig. 2) given by Eqs. (2a) and (3a) are strongly negative (i.e. the reactions are strongly exothermic) for both $MgSiO_3$ phases, resulting in the presence of Fe^{3+} and free metallic iron in the lower mantle. The counterintuitive coexistence of Fe^{3+} and metallic iron at high pressure was first considered by Mao in 1974 [28] and is feasible due to the high packing density of the iron metal phase, as well as compactness and stability of the Fe^{3+} ion with the half-filled d-electron shell.

Our simulations give evidence that this self-oxidization reaction will happen both in *Pv* and *PPv*, and in fact
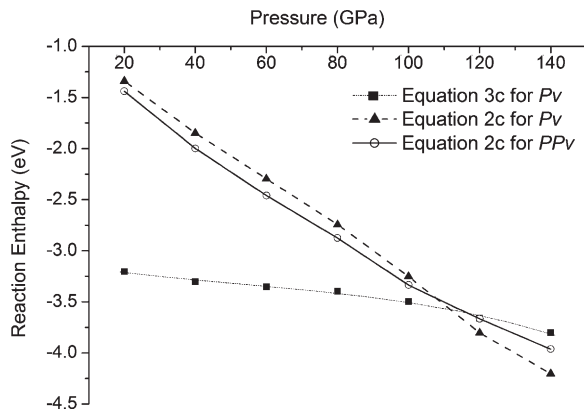
Fig. 2. Reaction enthalpies for Eq. (2c) (Al-free) and Eq. (3c) (Al-bearing system) as a function of pressure. Results for both Pv and PPv are shown. Valence disproportionation occurs in all these cases.

this reaction should take place even without the presence of Al^{3+} in the system. As a result, the lower mantle must be enriched in Fe^{3+} and have some free metallic iron[1], which (when molten) will gradually sink down to the Earth's core thus providing a possible mechanism for the growth of the Earth's core. A number of reactions have been proposed to take place between iron and mantle silicates [29,30] — typically, such reactions extract siderophiles, Si and possibly O into the iron metal; the ubiquitous presence of dispersed iron throughout the lower mantle would help equilibrating such reactions and could spread them far away from the core-mantle boundary. Gradual removal of metallic iron from the mantle into the core will leave the mantle enriched in oxygen and depleted in siderophiles and silicon. Removing metallic iron from the mantle could further pump Fe^{2+} from (Mg,Fe)O magnesiowüstite to Pv and PPv, where it would transform into Fe^{3+} and metal iron. Assuming that 60% of the pyrolitic amount of iron has undergone reaction (3b) during the Earth's history, we find the total amount of released heat to be quite significant, up to 5.0×10^{29} J, which would raise the temperature of the whole mantle by some 110 °C.

In Pv, the presence of Al^{3+} further increases the tendency of Fe^{2+} to disproportionate; in PPv the situation is different. For Pv we find that $[Fe^{3+}-Al^{3+}]$ coupled substitutions are favourable, in agreement with previous studies [2,3,8]. However, in PPv separate

$[Fe^{3+}-Fe^{3+}]$ and the $[Al^{3+}-Al^{3+}]$ coupled substitutions exist more stably than the $[Fe^{3+}-Al^{3+}]$ coupled substitution. Thus, incorporation of Al^{3+} can markedly increase the proportion of Fe^{3+} in $(MgFe)(SiAl)O_3$ Pv [1,2,3,8] relative to PPv. For example, at 120 GPa and 3000 K the Fe^{3+} partition coefficient for an Al-bearing system is $K = 4.8$, while in the Al-free system $K = 39$. The net effect of $[Fe^{3+}-Al^{3+}]$ on the Pv–PPv transition pressure is the decrease by 3 GPa for 3.125 mol% $FeAlO_3$. Fig. 3 shows the effects of Fe^{2+}, Fe^{3+} and Al^{3+} impurities on the Pv–PPv phase transition pressure. These results are consistent with previous suggestions [20,31,22] that addition of Al_2O_3 slightly increases this transition pressure, while FeO and Fe_2O_3 considerably reduce it. The shift of the Pv–PPv transition pressure due to impurities can be represented by the following numbers: $\frac{\partial P_{tr}}{\partial x_{FeO}} = -0.997$ GPa, $\frac{\partial P_{tr}}{\partial x_{Fe_2O_3}} = -3.904$ GPa, $\frac{\partial P_{tr}}{\partial x_{Al_2O_3}} = 0.950$ GPa, $\frac{\partial P_{tr}}{\partial x_{FeAlO_3}} = -0.866$ GPa (where P_{tr} is the transition pressure and x is the molar concentration of a component in percent).
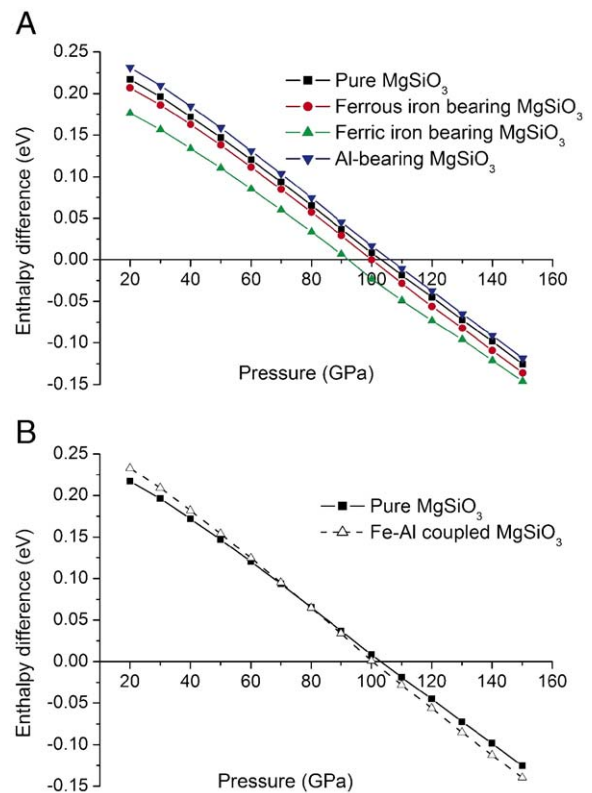

Fig. 3. Pv–PPv enthalpy difference as a function of chemistry and pressure. (A) Pure $MgSiO_3$, $(Mg,Fe)SiO_3$ with 3.125 mol% FeO, $(Mg, Fe)(Si,Fe)O_3$ with 3.125 mol% Fe_2O_3 and $(Mg,Al)(Si,Al)O_3$ with 3.125 mol% Al_2O_3. (B) $(Mg,Fe)(Si,Al)O_3$ with 3.125 mol% $FeAlO_3$, taking the most favourable coupled substitutions: $Fe^{3+}-Al^{3+}$ in Pv and $Fe^{3+}-Fe^{3+}$ and $Al^{3+}-Al^{3+}$ in PPv.

---

[1] The presence of metallic iron depends, however, on oxygen fugacity: when oxygen fugacity is sufficiently high, all iron can be converted to Fe^{3+} without the formation of metallic Fe. This possibility is interesting for further experimental and theoretical work. However in the deep mantle (especially close to the core) one expects very low oxygen fugacity and, thus, existence of metallic iron.

In the absence of Al^{3+}, the shortest $Fe^{3+}-Fe^{3+}$ distances are slightly longer in *PPv* than in *Pv* (at 100 GPa, 2.57 Å *vs* 2.51 Å) — thus, optical transparency will somewhat increase upon the formation of *PPv* in the Al-free system (in agreement with Ref. [4]). In the Al-bearing system, the shortest $Fe^{3+}-Fe^{3+}$ distance greatly increases in *Pv* (to 3.01 Å at 100 GPa), but remains the same in *PPv* (2.57 Å at 100 GPa). Therefore, aluminous *Pv* in the lower mantle will likely have a higher radiative conductivity than *PPv*. Thus we conclude that radiative conductivity cannot stabilize the D" layer against convection.

To analyse how temperature will affect our results, one needs a way to calculate the entropy and its magnetic, configurational and vibrational components. We take a simple approximation based on the electronic structure of the atoms, Stirling formula and equations of state of the minerals (see Supplementary material). For spin transitions of Fe^{3+}, there are three important effects of temperature: 1) shift of the HS–LS transition pressure, by ~ 7.7 MPa/K, 2) given the low concentration of impurities, the HS–LS transition is likely to be continuous rather than first-order at mantle temperatures [32], 3) gradual increase of the concentration of intermediate spin species (which is the highest entropy state for Fe^{3+} — Ref. [32]) with temperature. For Al-bearing *Pv* the HS–LS transition is predicted to occur at 134 GPa at 0 K; given the steep positive Clapeyron slope most of Fe^{3+} in the lower mantle and in the D" layer will be in the HS and IS states. For the reactions described by Eq. (2a) and Eq. (3a) we estimate a large negative entropy (ca -40 Jmol^{-1}K^{-1}), but this is not sufficient to change the direction of these reactions.

Concerning the discrepant results of previous studies [4,9,11] of the spin transition in Fe-bearing *Pv*, our results can help to find robust features in previous observations using Xray emission spectroscopy (XES) [4,9] and synchrotron Mössbauer spectroscopy (SMS) [11] techniques. These studies also differed in the composition of the samples and their treatment: Badro et al. [4] studied Al-free samples using laser heating to anneal the samples, while no laser heating was used in the works of Li et al. [9] on Al-bearing and Al-free *Pv* and Jackson et al. [11] on Al-free *Pv*. These differences explain much of the controversy between the results. First, the spin transition can occur only for Fe^{3+} (not Fe^{2+}), and large amounts of $Fe^{3+}(\sim 40\%$ of the total iron content according to Ref. [11]) are produced already during synthesis of *Pv* at high temperatures. With increasing pressure, according to our calculations the ratio $Fe^{3+}/\Sigma Fe$ should increase if the sample is thermally equilibrated (e.g. by laser heating), or remain

constant (as observed in Ref. [11]) if room-temperature compression is performed. At low concentrations of Fe^{3+}, the spin transition occurs of Fe^{3+} around 70 GPa [4,11] — or 76 GPa from our calculations. Second, in agreement with Li et al. [9] we find that incorporation of Al^{3+} greatly increases the spin transition pressure of Fe^{3+} ions — according to our results, from 76 GPa to 134 GPa. Furthermore, recent calculations [10] found that the spin transition pressure is very sensitive to the details of $Fe^{3+}-Al^{3+}$ distribution. The existence of many different local configurations in a solid solution makes continuous spin transitions in a wide pressure range possible even at low temperatures. Two previously reported experimental features remain controversial and difficult to explain — the two-stage spin transition of Ref. [4] (we can explain only the first transition at 70 GPa, but not the second one at 120 GPa), and the incompleteness of the spin transition in Ref. [9] even for an Al-free sample. Perhaps the most important point is that, comparing the spin transition pressures in Al-free (76 GPa) and Al-bearing *Pv* (134 GPa), we can conclude that Al-free samples are poor analogues of mantle *Pv*, due to strong $Al^{3+}-Fe^{3+}$ coupling in the *Pv* structure.

4. Conclusions

The valence and spin states of iron impurities have direct influence on the physical properties and chemical behavior of its host phase. This is important for the interpretation of seismic observations, geochemical models, and geodynamic simulation of the Earth's deep interior. At lower mantle conditions, it is energetically favorable for Fe^{2+} in *Pv* and *PPv* to "self-oxidize" by the reaction $3Fe^{2+} \rightarrow Fe(metal) + 2Fe^{3+}$ without needing external oxygen pump and leading to the formation of free iron metal phase. We have performed the first theoretical study of this reaction and, quite surprisingly, found it to be strongly exothermic. The favourability of this reaction is in line with previous experimental findings [3,5] and brings a new insight into the redox state of the inaccessible Earth's interior and into the mechanism of the Earth's core growth. Partial spin collapse of Fe^{3+} in *Pv* and *PPv* would significantly modify the properties of these minerals and here we have obtained a detailed and unified picture of these transitions. All these aspects are relevant for such properties as elasticity (especially for the shear moduli), thermal [4] and electrical conductivity and rheological properties of mantle minerals and warrant fruitful future research. Our results imply that at mantle conditions *PPv* should have lower radiative conductivity than *Pv* and, therefore, it is unlikely that radiative conductivity can

stabilize the D" layer against convection. The D" layer could, nevertheless, be nonconvecting if it is sufficiently compositionally different from the rest of the lower mantle. Finally, for the first time we have computationally studied the effect of Fe^{3+} incorporation on the *Pv–PPv* transition pressure and found that incorporation of Fe^{3+} lowers this transition pressure.

Until recently, the Earth's lower mantle was believed to be a simple region (both seismically and mineralogically). With the discoveries of new seismic features [33] and new mineral phases [6,7] the situation begins to change. Studies of the additional complexities brought about by the various forms of iron incorporation in mantle minerals, with a variety of valence and spin states, will certainly provide new insights into the dynamics and evolution of our planet.

Acknowledgements

Appendix A. Supplementary material

Supplementary data associated with this article can be found, in the online version, at doi:10.1016/j.epsl.2006.07.023.

References

[1] B.J. Wood, D.C. Rubie, The effect of alumina on the phase transformations at the 660-kilometer discontinuity from Fe–Mg partitioning experiments, Science 273 (1996) 1522–1524.

[2] C. McCammon, Perovskite as a possible sink for ferric iron in the lower mantle, Nature 387 (1997) 694–696.

[3] S. Lauterbach, C.A. McCammon, P.v. Aken, F. Langenhorst, F. Seifert, Mössbauer and ELNES spectroscopy of (Mg,Fe)(Si,Al) O_3 perovskite: a highly oxidised component of the lower mantle, Contrib. Mineral. Petrol. 138 (2000) 17–26.

[4] J. Badro, et al., Electronic transitions in perovskite: possible nonconvecting layers in the lower mantle, Science 305 (2004) 383–386.

[5] D.J. Frost, et al., Experimental evidence for the existence of iron-rich metal in the Earth's lower mantle, Nature 428 (2004) 409–412.

[6] M. Murakami, K. Hirose, K. Kawamura, N. Sata, F. Ohishi, Post-perovskite phase transition in $MgSiO_3$, Science 307 (2004) 855–858.

[7] A.R. Oganov, S. Ono, Theoretical and experimental evidence for a post-perovskite phase of $MgSiO_3$ in Earth's D″ layer, Nature 430 (2004) 445–448.

[8] D.J. Frost, F. Langenhorst, The effect of Al_2O_3 on Fe–Mg partitioning between magnesiowüstite and magnesium silicate perovskite, Earth Planet. Sci. Lett. 199 (2002) 227–241.

[9] J. Li, et al., Electronic spin state of iron in lower mantle perovskite, Proc. Natl. Acad. Sci. U. S. A. 101 (2004) 14027–14030.

[10] L. Li, et al., Electronic spin state of ferric iron in Al-bearing perovskite in the lower mantle, Geophys. Res. Lett. 32 (2005) L17307.

[11] J.M. Jackson, et al., A synchrotron Mossbauer spectroscopy study of (Mg,Fe)SiO_3 perovskite up to 120 GPa, Am. Mineral. 90 (2005) 199–205.

[12] R. Sinmyo, K. Hirose, H.St.C. O'Neil, E. Okunishi, Fe^{3+} in Al-bearing posterovskite phase, Geophys. Res. Lett. (2006) (under review).

[13] J.P. Perdew, K. Burke, M. Ernzerhof, M. Generalized gradient approximation made simple, Phys. Rev. Lett. 77 (1996) 3865–3868.

[14] P.E. Blöchl, Projector augmented-wave method, Phys. Rev., B 50 (1994) 17953–17979.

[15] G. Kresse, D. Joubert, From ultrasoft pseudopotentials to the projector augmented-wave method, Phys. Rev., B 59 (1999) 1758–1775.

[16] G. Kresse, J. Furthmüller, Efficiency of ab initio total-energy calculations for metals and semiconductors using a plane-wave basis set, Comp. Mater. Sci. 6 (1996) 15–50.

[17] R.E. Cohen, I.I. Mazin, D.G. Isaak, Magnetic collapse in transition metal oxides at high pressure; implications for the Earth, Science 275 (1997) 654–657.

[18] S.L. Dudarev, G.A. Botton, S.Y. Savrasov, C.J. Humphreys, A.P. Sutton, Electron-energy-loss spectra and the structural stability of nickel oxide: an LSDA+U study, Phys. Rev., B 57 (1998) 1505.

[19] J.P. Brodholt, Pressure-induced changes in the compression mechanism of aluminous perovskite in the Earth's mantle, Nature 407 (2000) 620–622.

[20] A.R. Oganov, S. Ono, The high-pressure phase of alumina and implications for Earth's D" layer, Proc. Natl. Acad. Sci. U. S. A. 102 (2005) 10828–10831.

[21] S. Ono, A.R. Oganov, In situ observation of phase transition between perovskite and $CaIrO_3$-type phase in $MgSiO_3$ and pyrolitic mantle composition, Earth Planet. Sci. Lett. 236 (2005) 914–932.

[22] R. Caracas, R.E. Cohen, Effect of chemistry on the stability and elasticity of the perovskite and post-perovskite phases in the $MgSiO_3$–$FeSiO_3$–Al_2O_3 system and implications for the lower-most mantle, Geophys. Res. Lett. 32 (2005) L16310.

[23] C.B. Vanpeteghem, R.J. Angel, N.L. Ross, S.D. Jacobsen, D.P Dobson, K.D. Litasov, E. Ohtani, Al, Fe substitution in the $MgSiO_3$ perovskite structure: a single-crystal X-ray diffraction study, Phys. Earth Planet. Inter. 155 (2006) 96–103.

[24] S. Stackhouse, J.P. Brodholt, D.P. Dobson, G.D. Price, Electronic spin transitions and the seismic properties of ferrous iron-bearing $MgSiO_3$ post-perovskite, Geophys. Res. Lett. 33 (2006) L12S03.

[25] K.J. Kingma, R.E. Cohen, R.J. Hemley, H.K. Mao, Transformation of stishovite to a denser phase at lower-mantle pressures, Nature 374 (1995) 243–245.

[26] L.S. Dubrovinsky, et al., Experimental and theoretical identification of a new high-pressure phase of silica, Nature 388 (1997) 362.

[27] O. Mathon, et al., Dynamics of the magnetic and structural α–ε phase transition in iron, Phys. Rev. Lett. 93 (2004) 255503.

[28] H.K. Mao, A discussion of the iron oxides at high pressure with implications for the chemical and thermal evolution of the earth, Carnegie Inst. 73 (1974) 510–518 (Washington Yearb).

[29] L. Dubrovinsky, et al., Iron-silica interaction at extreme conditions and the electrically conducting layer at the base of Earth's mantle, Nature 422 (2003) 58–61.

[30] E. Knittle, R. Jeanloz, Earth's core-mantle boundary: results of experiments at high pressures and temperatures, Science 251 (1991) 1438–1443.

[31] W.L. Mao, et al., Ferromagnesian postperovskite silicates in the D" layer of the Earth, Proc. Natl. Acad. Sci. 101 (2004) 15867–15869.

[32] W. Sturhahn, J.M. Jackson, J.-F. Lin, The spin state of iron in minerals of Earth's lower mantle, Geophys. Res. Lett. 32 (2005) L12307.

[33] J. Hernlund, C. Thomas, P.J. Tackley, A doubling of the post-perovskite phase boundary and structure of the Earth's lower-most mantle, Nature 434 (2005) 882–886.